

Article

Real-Time Experimental Monitoring for Water Absorption Evolution Behaviors of Sandstone in Mogao Grottoes, China

Nai Hao ^{1,2}, Yongliang Wang ^{1,2,*} , Xiaochong Wu ², Yifeng Duan ², Panshun Li ² and Manchao He ^{1,*}

¹ State Key Laboratory for Geomechanics and Deep Underground Engineering, China University of Mining and Technology (Beijing), Beijing 100083, China

² School of Mechanics and Civil Engineering, China University of Mining and Technology (Beijing), Beijing 100083, China

* Correspondence: wangyl@cumb.edu.cn (Y.W.); hemanhao@263.net (M.H.)

Abstract: Rock mass has typical pore structure, and the induced coupling effects of fluid and solid matrix appear in the disaster evolution process of deep energy exploitation and overground rock hydration. As a representative case, influenced by the water absorption environment, the surrounding rock and murals of Mogao Grottoes produce hydration diseases, which may be related to unclear interaction mechanisms between the surrounding rock and water. In this study, the self-developed physical experimental system for real-time experimental monitoring was applied to test the water absorption evolution behaviors of sandstone. The experimental results showed that the water evaporation of the rock sample during the process of water absorption could be measured through this well-designed physical experimental system, and the actual water absorption of the rock sample is the difference between the decrease of water in the water storage bucket, measured by the balance and the water evaporation in the process of experiment; by drawing the actual water absorption curve of the rock sample, the time when the water absorption of the rock sample reaches saturation could be determined accurately; and the curve of water absorption with time could be expressed as an exponential function. The experimental techniques and methods in this study provide a feasible research idea for studying the water absorption evolution behaviors and mechanisms of the surrounding rock weathering when it meets water, and have significance for revealing the disease mechanisms of the surrounding sandstone in Mogao Grottoes, China.

Keywords: sandstone; water absorption; time-dependent effect; experimental monitoring; rock mechanics



Citation: Hao, N.; Wang, Y.; Wu, X.; Duan, Y.; Li, P.; He, M. Real-Time Experimental Monitoring for Water Absorption Evolution Behaviors of Sandstone in Mogao Grottoes, China. *Energies* **2022**, *15*, 8504. <https://doi.org/10.3390/en15228504>

Academic Editor: Mohammad Sarmadivaleh

Received: 23 September 2022

Accepted: 8 November 2022

Published: 14 November 2022

Publisher's Note: MDPI stays neutral with regard to jurisdictional claims in published maps and institutional affiliations.



Copyright: © 2022 by the authors. Licensee MDPI, Basel, Switzerland. This article is an open access article distributed under the terms and conditions of the Creative Commons Attribution (CC BY) license (<https://creativecommons.org/licenses/by/4.0/>).

1. Introduction

Rock mass is involved in deep energy exploitation and overground rock structure, which is a typical porous medium and arises from the coupling effects of fluid and solid matrix in the disaster evolution process [1,2]. From a phenomenal point of view, clay minerals in argillaceous cements of rocks, such as montmorillonite and chlorite, repeatedly absorb water for expansion and shrinkage after hydration. Essentially, the mineral composition of rock matrix and water react chemically, leading to the destruction of the cementation structure of glutenite, which changes or even weakens the rock mechanical properties. The interaction between the rocks and water mentioned above makes rocks prone to various types of damage, forming various forms of hydration disasters. As a representative case, influenced by water-rock materials and water absorption environment, the surrounding rock and murals of Mogao Grottoes produce hydration diseases. Mogao Grottoes, Dunhuang, is a famous historical and cultural heritage site in China, which has significant scientific, artistic, historical, social and cultural values, and it is of great significance to protect the murals. The excavated rock mass is calcareous argillaceous or argillaceous weakly cemented gravel rock mass. The murals of Mogao Grottoes are composed of support, ground battle layer, powder layer and pigment layer. Affected by

natural and human factors, the murals produce a variety of diseases, mainly including armoring, caustic soda, hollowing, large-areas falling off the murals, mildew, etc. [3–5]. As a cultural relic, the salt damage of murals and the weathering of carrier gravel rock mass have become the two most direct factors threatening the long-term preservation of the Mogao Grottoes. Many studies have proved that these diseases are mainly caused by water and salt migration. The migration of water vapor in rock mass promotes the enrichment of salt on the surface of murals, which is one of the main reasons for cave diseases [6]. However, the behaviors of water absorption evolution and the migration of water vapor of sandstone have not been well understood and evaluated.

Some numerical simulations have been proposed to describe the water-rock interaction behavior and mechanisms. The water-rock interaction will reduce the shear strength of the fracture and thus deteriorate the stability of the slope. There are two main mechanisms for weakening rock fracture. The first is the hydrogeological process, in which the water pressure in the crack gap changes the effective normal stress acting on the crack wall; the second is the physicochemical factor, which reduces the cohesion and friction of cracks [7]. Ma et al. [8] established a one-dimensional radial three-phase flow model of water-rock-silt, and showed that with the development of three-phase flow, the rock particles near the fluid outlet are first fluidized and constantly migrate outward, resulting in the increase of porosity and permeability of fault rocks. Subsequently, water conducting channels are gradually formed in the fault rocks, and then more fluidized rock particles flow out. Finally, the fluidized rock particles have completely migrated, and the porosity and permeability tend to be stable, with a more significant uneven spatial distribution. Bi et al. [9] proposed a new numerical model, which shows that water pressure plays a key role in the stress field around the crack tip and the propagation path and coalescence mode of wing crack and secondary crack. Huang et al. [10] used the developed numerical program to evaluate the effect of anisotropic pore size on the flow channel and permeability of the fracture network. With the decrease of the average value and the increase of the deviation of the aperture field along the normal distribution, the localization of the fluid flow becomes more and more obvious [11].

In addition, some scholars have studied the water-rock interaction behavior, moisture content variation, and mechanism through physical experiments [12]. Ma et al. [13] studied the energy evolution law of gypsum rock with different soaking time under one-dimensional load, and proved that the input energy, elastic energy and dissipation energy all decreased with the increase of soaking time. Lin et al. [14] used nuclear magnetic resonance technology to measure the porosity and pore size distribution of sandstone samples immersed in different chemical solutions; the porosity and macropore ratio of sandstone increase after chemical corrosion. The attenuation laws of compressive strength and the tensile strength of sandstone under static and dynamic conditions are similar, and the relationship between them and damage variables is exponential. Dynamic tensile strength is most sensitive to chemical corrosion, further, Lin et al. [15] studied the effects of water content and stress level on creep strain, creep rate, long-term strength and creep failure mode. With the increase of water content, the long-term strength of rock decreases continuously; with the increase of water content, the rock shows the regularization of the main fracture surface, the number of secondary cracks gradually decreases, and the shear slip phenomenon observed gradually disappears. Besides, wetting-drying cycles and temperature change will also affect the mechanical properties of sandstone. During the successive wetting-drying cycles, Yao et al. [16] studied that the young's modulus and macroscopic mechanical strength, including uniaxial compressive strength and the tensile strength of sandstone, gradually decrease, while the abundance and complexity of sandstone pores tend to increase, and the physical structure of the internal part (i.e., density or porosity) is affected later than the physical structure of the sample surface. The two physical processes of cyclic wetting drying and cyclic cooling heating will degrade the sandstone, and the coupling of the two processes will accelerate the degradation rate of the sandstone. The larger the temperature change, the higher the deterioration rate of multi-scale physical and

mechanical properties of sandstone (including mineral composition, microstructure, pore size distribution characteristics, permeability and macro mechanical parameters) [17].

The interaction between water and grotto surrounding rock is important for the weathering of the surrounding rock and the occurrence of mural damage (especially salt damage). More on-site studies have been carried out above, and less experimental studies on water rock interaction have been carried out for the surrounding rock of Mogao Grottoes. In order to better protect the original site of the murals, more simulation tests should be carried out to minimize the damage to murals. To study the interaction between water and rock, the authors of this paper developed the real-time monitoring experimental system for water interaction of soft rock. The system adopts the mode of single-sided water absorption, and can realize two modes of water absorption without water pressure, and water absorption with water pressure. Systematic measures to reduce water evaporation are proposed, but the influence of water evaporation on rock water absorption is not determined quantitatively. However, the accurate determination of rock water absorption is of great significance for the study of rock permeability. At present, there are few studies on the water absorption characteristics of rock under certain pressure, and there is no distinction between the mechanical and physicochemical effects of water on rock. In the research of this paper, the experimental test technology of the real-time monitoring experimental system for water physical action of soft rock developed in previous studies [18–21] is improved, and by adding auxiliary equipment and a water absorption mode, the water absorption characteristics of the sandstone in Mogao Grottoes are tested; further, the influence of evaporation on the water absorption quality of rock samples is accurately and quantitatively evaluated, and the mechanical and physicochemical effects of water on rocks are quantitatively distinguished. The research results can provide a basic scientific basis for the prevention and control of surrounding rock weathering and mural salt damage. The structure of this paper is organized as follows. In Section 2, the experiment and procedures are introduced, containing the real-time monitoring experimental system and procedures, and the microstructure and components of sandstone samples in Mogao Grottoes, China; in Section 3, the results and analysis for interaction behaviors between water and sandstone are introduced; and in Section 4, the remarkable conclusions are summarized.

2. Experiment and Procedures

2.1. Real-Time Monitoring Experimental System and Procedures

The physical experimental system for real-time experimental monitoring includes a test box, a temperature and humidity sensor, one or more sets of adsorbed water test devices and a data collector. The physical experimental system for real-time experimental monitoring of water absorption evolution behaviors of sandstone in Mogao Grottoes, China, is shown in Figure 1, and the sketch for real-time monitoring experimental system for the imbibition test without water pressure is shown in Figure 2. The front of the test box is provided with an observation window, the rear end is provided with an operation platform, and the interior is provided with a partition plate. The temperature and humidity sensor are fixed at the front of the test chamber near the top, and they are used to detect the temperature and humidity information in the test chamber. The adsorbed water test device includes a pressurized adsorbed water device, a pressureless adsorbed water device and an electronic balance. The electronic balance corresponds to the pressurized adsorbed water device and the pressureless adsorbed water device, respectively. The electronic balance, the pressurized adsorbed water device and the pressureless adsorbed water device are placed on the diaphragm, respectively, and the pressurized adsorbed water device and the pressureless adsorbed water device correspond to the observation window, respectively. The data collector is connected outside the test chamber, receives the reading information of the temperature and humidity sensor and electronic balance, and draws the test chart.



Figure 1. Physical experimental system for real-time experimental monitoring for water absorption evolution behaviors of sandstone in Mogao Grottoes, China.

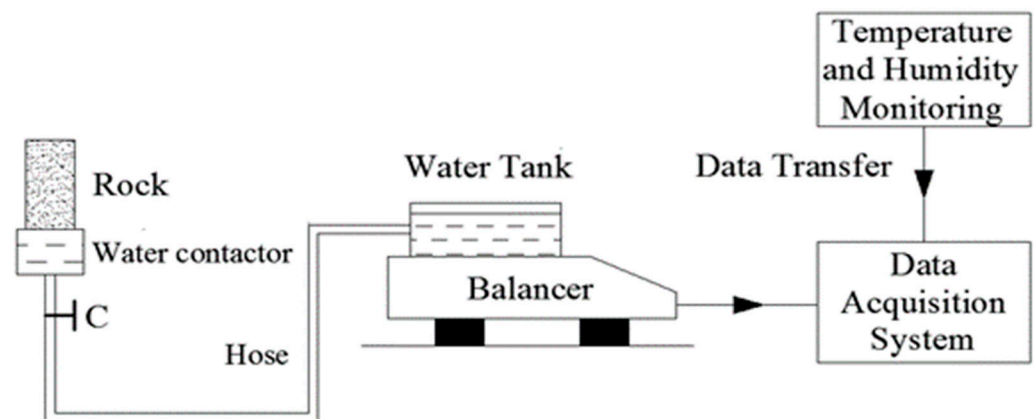


Figure 2. Sketch for real-time monitoring experimental system for imbibition test without water pressure.

The pressurized adsorption water device comprises a water storage bucket and a pressurized water contactor. The water storage bucket is placed on the corresponding electronic balance, the pressurized water contactor is connected with the water storage bucket pipeline, and the horizontal position of the water storage bucket is higher than the pressurized water contactor. The pressure water contactor is an inverted cup-shaped structure, the top of the cup-shaped structure is provided with a water inlet and an exhaust port, the water inlet and the exhaust port are respectively provided with valves, and the water inlet is connected with the water storage bucket through a pipe. The pressureless adsorption water device comprises a water storage bucket and a pressureless water contactor; the water storage bucket is placed on the corresponding electronic balance; the pressureless water contactor is connected with the water storage bucket pipe; the horizontal position of the water storage bucket is flush with the pressureless water contactor. The pressureless water contactor is a cup-shaped structure; an annular support surface is arranged on the inner wall near the top of the cup-shaped structure; a water inlet is arranged at the bottom of the cup-shaped structure; a valve is arranged on the water inlet; the water inlet is connected with the water storage bucket in the corresponding pressureless adsorption water device.

The electronic balance is also provided with a sealing cover; the water storage bucket is placed in the sealing cover; the data collector is a computer with relevant software.

The real-time monitoring experimental procedures for the imbibition test without water pressure is shown in Figure 3. The steps and scheme of experimental operation in this study can be summarized as follows:

- (1) Firstly, open the rear operation interface of the test box, inject water into each water storage bucket to three-quarters of the volume, and fill the connecting pipe.
- (2) Secondly, open the valve on the water inlet of the pressureless water contactor to fill the water storage area of the pressureless water contactor.
- (3) Thirdly, the glass mold (no water absorption) with the same diameter as the experimental non pressure rock sample is placed on the support surface of one non pressure water contactor, and three pressureless rock samples are placed on the support surface of three pressureless water contactors. The water absorption end of the pressureless rock sample contacts the water surface of the water storage area, and the water absorption process of the pressureless rock sample begins.
- (4) Finally, close the observation window, turn on the computer for data acquisition, collect the reading information on each electronic balance and temperature and humidity sensor at any time, and automatically draw the test chart after summary and analysis to record the process of adsorbed water of each rock sample.

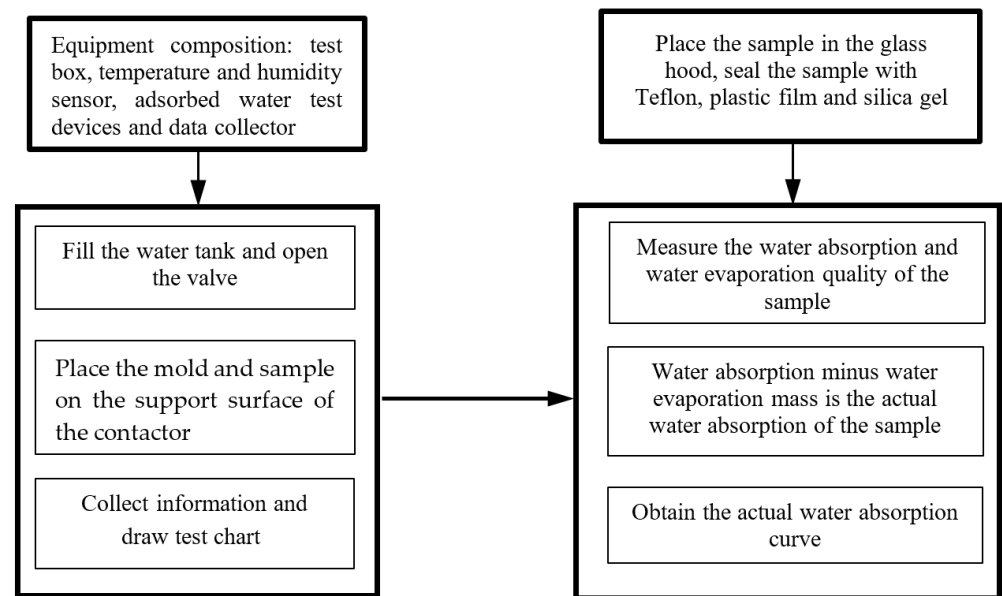


Figure 3. Real-time monitoring experimental procedures for imbibition test without water pressure.

2.2. Microstructure and Components of Sandstone Samples in Mogao Grottoes, China

(1) XRD experimental results of sandstone samples

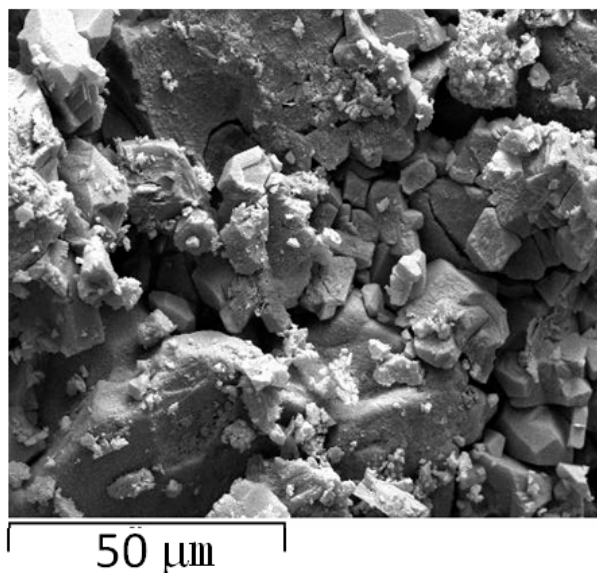
The sandstone sample is taken from the north area of Mogao Grottoes, China. The color is gray white, and the section is rough. The XRD (X-ray diffraction) results are shown in Table 1, which shows that the main mineral components of sandstone are quartz and calcite, followed by dolomite, albite and potassium feldspar. The total amount of clay minerals in sandstone is 29.7%, of which illite accounts for 68%, kaolinite for 8% and chlorite for 24%.

(2) SEM experimental results of sandstone samples

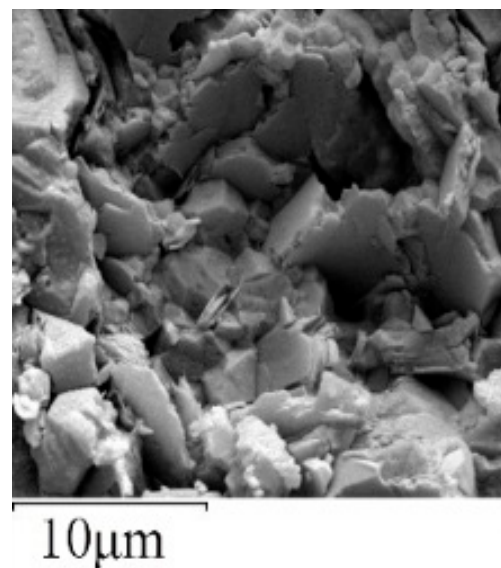
The SEM (Scanning Electron Microscope) image of the sample is shown in Figure 4. It can be seen from the observation that the inter particle pore distance is mainly between 10–20 μm at 1200 times magnification, and more flake illite is found at 5000 times magnification.

Table 1. XRD experimental results of sandstone samples.

Quartz	Potash Feldspar	Minerals (%)			Clay Minerals	Clay Minerals (%)		
		Soda Feldspar	Calcite	Dolomite		Illite	Kaolinite	Chlorite
24.3	0.5	6.3	22.8	16.4	29.7	68	8	24



(a) Magnified micrograph by 1200 times



(b) Magnified micrograph by 5000 times

Figure 4. SEM experimental results of sandstone samples.

(3) Mercury intrusion test results

The basic characteristic parameters of the pore structure of rock samples measured by the mercury injection experiment are shown in Table 2. To simulate the capillary action of water and the water absorption characteristics of rock, water and rock are mainly physical and chemical actions materials. Three samples are placed in each group, and a cylindrical glass mold with a diameter of 50 mm and a height of 100 mm is placed in one window to measure the water evaporation quality during the experiments. The water absorption curve of each sample is measured, and the corresponding water absorption at each time minus the evaporation at the same time is the actual water absorption of the sample, so as to obtain the actual water absorption curve. The inner diameter of the water contact is 70 mm and the diameter of the rock sample is 50 mm. Therefore, when the sample is placed on the built-in diaphragm of the water contact, there is an annular water surface with a width of 10 mm around the rock sample. The annular water surface will evaporate all the time during the test, and the quality of the evaporated water is also the source of data increase in the data acquisition system. At the same time, the evaporation of water in the water storage bucket should also be considered. If we ignore the quality of the evaporated water, the water absorption of the rock sample is equal to the data collected by the balance. However, we cannot ignore the water evaporation, because the water evaporation is not small enough compared with the water absorption of the rock sample. Especially when the water absorption process lasts for a long time, even if we place the sample in the glass hood to reduce the water evaporation, but we still cannot completely avoid the evaporation of water in such experiments.

The sample shall be wrapped around with Teflon; the upper end face shall be wrapped with plastic film, and the upper end face shall be sealed with silica gel to avoid water evaporation on the sample surface during water absorption. Then, the sample shall be placed on the water contactor, and the bottom surface of the sample shall be in contact with

the water surface. In order to analyze the evaporation of water, we place a cylindrical mold made of glass on the water contactor in a window, with a diameter of 50 mm and a height of 100 mm. Because the glass mold itself does not absorb water, the data collected by the balance connected with the water contactor below is the evaporation of water during the test. The parameters of sandstone samples in the imbibition test without water pressure (capillary effects) are shown in Table 3.

Table 2. Basic pore parameters of sandstone samples.

Porosity (%)	Specific Surface Area (m ² /g)	Volume Median Pore Diameter (nm)	Area Median Pore Diameter (nm)	Mean Pore Diameter (nm)	Bulk Density (g/mL)	Skeleton Density (g/mL)
12.23	0.082	9764.8	974.4	2838.4	2.11	2.41

Table 3. Parameters of sandstone samples in imbibition test without water pressure (capillary effects).

Group	Sample	Diameter <i>d</i> (mm)	Length <i>l</i> (mm)	Dried Mass before Test <i>M</i> ₁ (g)
A	FS4	49.52	91.08	406.432
A	FS11	50.00	92.12	414.024
A	FS12	49.56	94.20	406.400
B	FS1	48.36	101.14	449.706
B	FS13	49.38	92.48	399.947
B	FS14	49.38	97.58	425.623
Average		49.37	94.77	417.022

3. Results and Analysis for Interaction Behaviors between Water and Sandstone

Using the above experimental system and sandstone samples in Group A and B, the environmental temperature and humidity during the imbibition test without water pressure is shown in Figure 5. It can be observed that the environmental temperature (*T* (°C)) is basically maintained at 24.5 °C and humidity (RH (%)) is basically maintained at 25.5% during the whole test process.

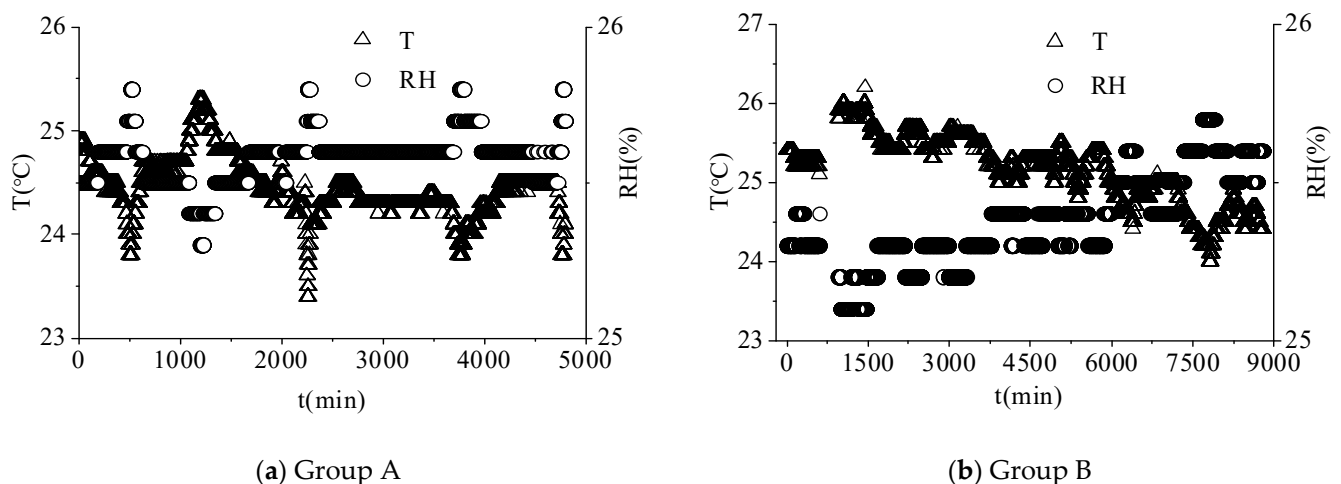


Figure 5. Environmental temperature and humidity during imbibition test without water pressure.

The relationship between water imbibition and time during the imbibition test without water pressure is shown in Figure 6. In the initial stage, water absorption increases rapidly, and gradually slowed down with the increase of time. When the water absorption time is long enough, water absorption tends to remain constant. The measured value of water reduction in the water storage bucket measured is Q_2 (measured water), as shown in the curve with triangles, water evaporation Q_1 (evaporated water), as shown in the curve with

circulars, and the actual water absorption of rock sample Q_3 (absorbed water), as shown in the curve with squares. Therefore, the relation of these three can be expressed as:

$$Q_3 = Q_2 - Q_1 \tag{1}$$

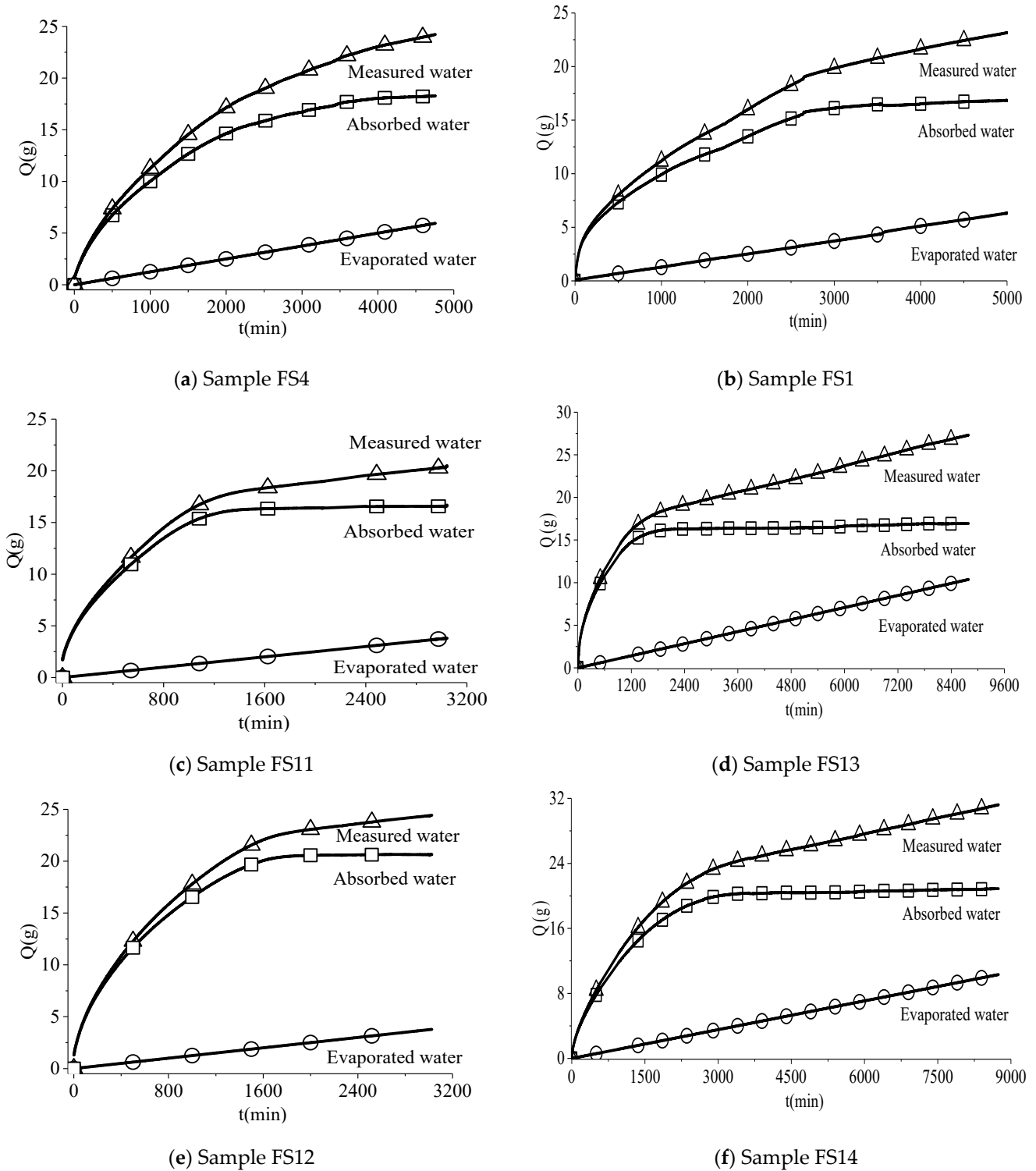


Figure 6. Relationship between water imbibition and time during imbibition test without water pressure.

Figure 6 shows the relationship between water imbibition and time during the imbibition test without water pressure. As shown in Figure 6, with the change of time, the water absorption of rock samples has experienced three stages: rapid growth, gradual slowing down and tending to be constant. As shown in Figure 6a,c,e, the three rock samples FS4, FS11 and FS12 of Group A tend to be constant at 4000 min, 1400 min and 2000 min, respectively; as shown in Figure 6b,d,f, the three rock samples FS1, FS13 and FS14 of Group B tend to be constant at 3000 min, 1800 min and 3000 min, respectively. Actually, under the condition of a certain temperature and humidity, the water evaporation is proportional to the time, and the evaporation is always increasing; in the implementation of the experiment, the volume of rock samples in this study is fixed and limited; after the water absorption of rock samples reaches saturation at a certain time, the water absorption will not increase, so the curve shown in Figure 6 shows that the water absorption is constant. In order to compare the relative size of water absorption of the samples, we draw the curves of water absorption and water absorption, as shown in Figures 7 and 8, respectively. The index function shown in Equation (2) was used to fit the water absorption data points, and the results of fitting curve parameters were shown in Table 4.

$$w(t) = a \cdot \exp(t/p) + w \quad (2)$$

where a , b , and w are parameters, t is time. By comparing the results in Figure 8 and Table 4, they show that the water absorption of the three samples has the same change trend. Since the water content of the rock sample is low at the initial stage and the water absorption rate is fast, the water absorption of the rock sample increases rapidly. Subsequently, as the pores of the rock sample are continuously filled with water, the water absorption rate gradually decreases and the water absorption slowly increases. Finally, as the pores of the rock samples are saturated with water, the water absorption tends to be stable. Hence, the water absorption curve can be fitted by exponential function.

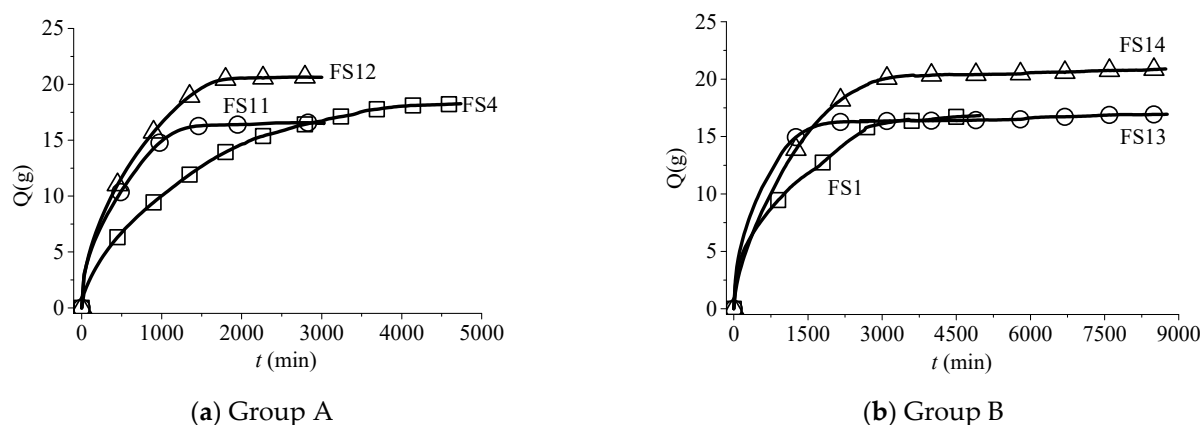


Figure 7. Relationship between water imbibition and time.

The quality changes of samples before and after water absorption were counted, and the results were shown in Table 5. In Table 5, the water evaporation is derived by the water tank and the evaporation of water quality; water loss of the water tank represents the reduction of water mass measured by the electronic balance carrying the water tank; automatic measurement of water quality represents the water loss mass of water tank minus water evaporation mass; manual measurement of water absorption represents the mass of the sample containing water minus the dry mass of the sample before water absorption. The water absorption rate represents the ratio of manually measured water absorption to the drying quality of the sample before water absorption. According to Table 5, automatic measurement of water absorption quality is close to manual measurement of water absorption quality after considering water evaporation effect.

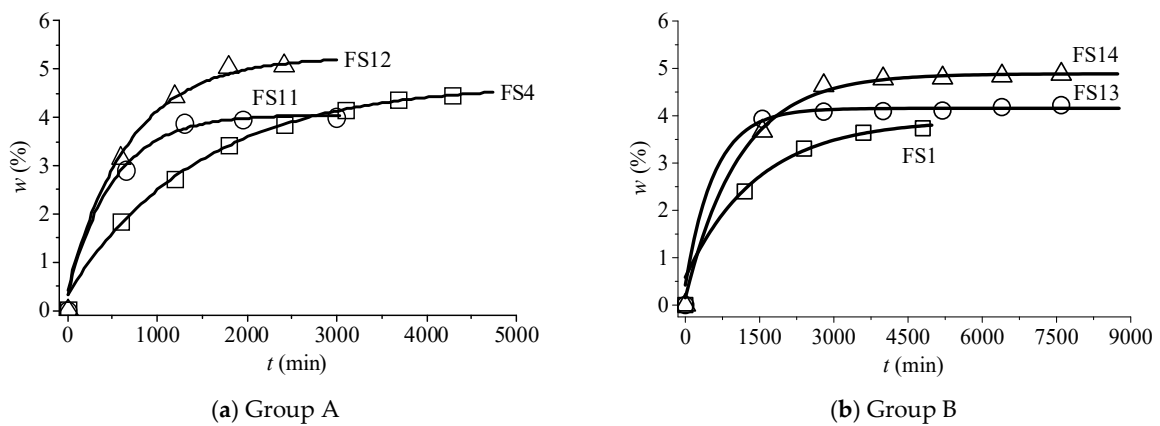


Figure 8. Relationship between water imbibition content and time.

Table 4. Fitting results of parameters during imbibition test (R^2 is the correlation coefficient).

Sample	Fitting Parameters				Sample	Fitting Parameters			
	a	b	w	R^2		a	b	w	R^2
FS-4	-4.341	-1477.740	4.704	0.999	FS-1	-3.326	-1465.154	3.912	0.990
FS-11	-3.638	-529.384	4.072	0.993	FS-13	-3.7323	-587.070	4.156	0.992
FS-12	-4.770	-698.107	5.267	0.995	FS-14	-4.7311	-1101.379	4.886	0.996

Table 5. Results of imbibition test without water pressure.

Group	Sample	Time t (min)	Water Quality Evaporated Q1 (g)	Water Quality Reduced Q2 (g)	Imbibition Measured Automatically Q3 (g)	Dried Mass before Test M1 (g)	Hydrous Mass after Test M2 (g)	Imbibition Measured Manually M3 (g)	Imbibition Error E (%)	Water Content w (%)
A	FS4	4755	5.94	24.22	18.28	406.432	424.459	18.027	1.40	4.44
	FS11	3042	3.80	20.50	16.70	414.024	429.585	15.561	7.32	3.76
	FS12	3024	3.78	24.43	20.65	406.400	427.198	20.798	-0.71	5.12
B	FS1	4999	6.32	23.16	16.84	449.706	466.144	16.438	2.45	3.66
	FS13	8792	10.375	27.32	16.945	399.947	416.887	16.940	0.03	4.24
	FS14	8745	10.319	31.210	20.891	425.623	448.369	22.746	-8.16	5.34

The hydration damage and disaster of the rock are related to the hydration behavior of each component in rock. The sandstone sample used in this study reaches the saturation state at the end of the experiment, as shown in Figure 9 below; the sandstone sample has no significant hydration damage at the same time as the initial time. Other rock samples (i.e., mudstone) may suffer from hydration damage and failure, due to different compositions of rock matrix. This will be studied in the next study.



Figure 9. Sandstone samples used in this study reaches the saturation state at the end of the experiment.

4. Conclusions

This paper studies the water absorption evolution behaviors of sandstone in Mogao Grottoes, China, using real-time experimental monitoring, and the conclusions can be summarized as follows:

- (1) The physical experimental system for real-time experimental monitoring for water absorption evolution behaviors is developed. This experimental system simulates three modes of rock sample water absorption process under the action of capillary, gravity and hydrostatic pressure, and accurately estimates the water absorption quality of rock samples, environmental temperature and humidity, in real time.
- (2) The effects of water evaporation on the water absorption quality of the rock samples are evaluated quantitatively and accurately. The actual water absorption of the rock samples should be the difference between the amount of water reduction measured by the balance and the amount of water evaporation. The quantitative value of water in rock mass is measured by the developed experiments.
- (3) The water absorption process of sandstone in Mogao Grottoes, China, under capillary action is simulated by a non-pressure water absorption experiment. The water absorption characteristic curve of the rock samples can be fitted by exponential function, and it shows that the water absorption increases rapidly in the initial stage, then slowly increases, and finally tends to be stable. These results can provide reference for evaluating hydration and protecting rock mass.

This research has carried out water absorption tests on the basis of laboratory experiments, and analyzed damage behaviors related to water salt migration from the perspective of rock water absorption. However, the weathering of surrounding rock and the salt damage of murals caused by water salt migration are a very complex process, and the water rock interaction behavior and mechanism under different temperature, humidity and multi field coupling conditions, are important research topics in the future. In addition, the experimental system and procedures used in this study can also be extended to the analysis of water-rock interaction of rock mass in deep ground energy exploitation; how to apply in situ stresses and pore water pressure is the focus of the next stage of research.

Author Contributions: N.H., Y.W. and M.H., conceptualization, methodology, resources, writing—reviewing and editing, supervision, project administration, funding acquisition; X.W., Y.D. and P.L., methodology, software, formal analysis, investigation, data curation, writing—original draft preparation, visualization. All authors have read and agreed to the published version of the manuscript.

Funding: The authors gratefully acknowledge financial support from the Open Fund of State Key Laboratory for GeoMechanics and Deep Underground Engineering, China University of Mining and Technology (Beijing) (grant SKLGDUEK202209), Fundamental Research Funds for the Central Universities (grant 2021YQSB04), Innovation Training Program for College Students (grant 202106036), National Natural Science Foundation of China (grant 41877275), Beijing Natural Science Foundation (grant L212016), Yue Qi Young Scholar Project Foundation of China University of Mining and Technology (Beijing) (grant 2019QN14).

Data Availability Statement: Not applicable.

Conflicts of Interest: The authors declare no conflict of interest.

References

1. Wang, Y.; Wang, J.; Li, L. Dynamic propagation behaviors of hydraulic fracture networks considering hydro-mechanical coupling effects in tight oil and gas reservoirs: A multi-thread parallel computation method. *Comput. Geotech.* **2022**, *152*, 105016. [[CrossRef](#)]
2. Wang, Y. *Adaptive Analysis of Damage and Fracture in Rock with Multiphysical Fields Coupling*; Springer Press: Berlin/Heidelberg, Germany, 2021.
3. Wang, X.; Fu, P. Summary of painting materials and techniques of the Mogao Grottoes. Mural paintings of the Silk Road: Cultural exchanges between East and West. In Proceedings of the 29th Annual International Symposium on the Conservation and Restoration of Cultural Property, National Research Institute for Cultural Properties, Tokyo, Japan, 19–21 January 2007.

4. Agnew, N.; Maekawa, S.; Wei, S. Causes and mechanisms of deterioration and damage in Cave 85. Conservation of Ancient Sites on the Silk Road. In Proceedings of the Second International Conference on the Conservation of Grotto Sites, Mogao Grottoes, Dunhuang, China, 28 June–3 July 2004; Agnew, N., Ed.; Getty Conservation Institute: Los Angeles, CA, USA, 2010; pp. 412–420.
5. Guo, Q.; Wang, X.; Zhang, H.; Li, Z.; Yang, S. Damage and conservation of the high cliff on the Northern area of Dunhuang Mogao Grottoes, China. *Landslides* **2009**, *6*, 89–100. [[CrossRef](#)]
6. Li, H.; Wang, W.; Zhan, H.; Qiu, F.; Guo, Q.; Zhang, G. Water in the Mogao Grottoes, China: Where it comes from and how it is driven. *J. Arid. Land* **2015**, *7*, 37–45. [[CrossRef](#)]
7. Zhao, Z.; Guo, T.; Ning, Z.; Dou, Z.; Dai, F.; Yang, Q. Numerical modeling of stability of fractured reservoir bank slopes subjected to water–rock interactions. *Rock Mech. Rock Eng.* **2020**, *53*, 2215–2231. [[CrossRef](#)]
8. Ma, D.; Duan, H.; Zhang, J.; Liu, X.; Li, Z. Numerical simulation of water–silt inrush hazard of fault rock: A three-phase flow model. *Rock Mech. Rock Eng.* **2022**, *55*, 5163–5182. [[CrossRef](#)]
9. Bi, J.; Zhou, X. A novel numerical algorithm for simulation of initiation, propagation and coalescence of flaws subject to internal fluid pressure and vertical stress in the framework of general particle dynamics. *Rock Mech. Rock Eng.* **2017**, *50*, 1833–1849. [[CrossRef](#)]
10. Huang, N.; Jiang, Y.; Liu, R.; Li, B. Experimental and numerical studies of the hydraulic properties of three-dimensional fracture networks with spatially distributed apertures. *Rock Mech. Rock Eng.* **2019**, *52*, 4731–4746. [[CrossRef](#)]
11. Ren, Q.; Jin, Q.; Feng, J.; Li, M.; Du, H. Mineral filling mechanism in complex carbonate reservoir fracture system: Enlightenment from numerical simulation of water–rock interaction. *Rock Mech. Rock Eng.* **2020**, *195*, 107769. [[CrossRef](#)]
12. Al-Khailany, D.K.; Saleh, M.M.; Daraei, A. Evaluating the Moisture Content Variation on Critical Strain of Geo-materials: A Case Study. *J. Eng.* **2022**, *28*, 27–38. [[CrossRef](#)]
13. Ma, H.; Song, Y.; Chen, S.; Yin, D.; Zheng, J.; Shen, F.; Li, X.; Ma, Q. Experimental investigation on the mechanical behavior and damage evolution mechanism of water-immersed gypsum rock. *Rock Mech. Rock Eng.* **2021**, *54*, 4929–4948. [[CrossRef](#)]
14. Lin, Y.; Zhou, K.; Li, J.; Ke, B.; Gao, R. Weakening laws of mechanical properties of sandstone under the effect of chemical corrosion. *Rock Mech. Rock Eng.* **2020**, *53*, 1857–1877. [[CrossRef](#)]
15. Lin, H.; Zhang, Q.; Zhang, L.; Duan, K.; Xue, T.; Fan, Q. The influence of water content on the time-dependent mechanical behavior of argillaceous siltstone. *Rock Mech. Rock Eng.* **2022**, *55*, 3939–3957. [[CrossRef](#)]
16. Yao, W.; Li, C.; Zhan, H.; Zhou, J.; Criss, R.; Xiong, S.; Jiang, X. Multiscale study of physical and mechanical properties of sandstone in three gorges reservoir region subjected to cyclic wetting–drying of yangtze river water. *Rock Mech. Rock Eng.* **2020**, *53*, 2215–2231. [[CrossRef](#)]
17. Zhang, C.; Dai, Z.; Tian, W.; Yang, Y.; Zhang, L. Multiscale study of the deterioration of sandstone in the three gorges reservoir area subjected to cyclic wetting–cooling and drying–heating. *Rock Mech. Rock Eng.* **2022**, *55*, 5619–5637. [[CrossRef](#)]
18. He, M.; Sun, X.; Zhao, J. Advances in interaction mechanism of water (gas) on clay minerals in China. *Int. J. Min. Sci. Technol.* **2014**, *24*, 727–735. [[CrossRef](#)]
19. He, M.; Zhang, N. Experimental study on water absorption and strength degradation effect of shale at great depth. *Dis. Adv.* **2014**, *7*, 28–36.
20. Guo, H.; He, M.; Sun, C.; Li, B.; Zhang, F. Hydrophilic and strength-softening characteristics of calcareous shale in deep mines. *J. Rock Mech. Geotech. Eng.* **2012**, *4*, 344–351. [[CrossRef](#)]
21. Li, D.; Wang, G.; Han, L.; Liu, P.; He, M.; Yang, G.; Tai, Q.; Chen, C. Analysis of microscopic pore structures of rocks before and after water absorption. *Min. Sci. Technol.* **2011**, *21*, 287–293.